International Journal of Operations Research

International Journal of Operations Research Vol. 3, No. 1, 56−75 (2006)

Development of Confidence Interval and Hypothesis Testing for Taguchi Capability Index Using a Bayesian Approach

Shu-Kai S. Fan* and Ching-Kuei Kao

Department of Industrial Engineering and Management, Yuan Ze University, Taoyuan County, 320, Taiwan, R.O.C.

Abstract—Process capability indices are designed to describe how the process of interest can achieve to meet specification limits under a condition of statistical control. One of the capability indices is denoted as C_{pm} proposed by Chan, Cheng and Spiring (1988), sometimes termed the Taguchi index. The primary goal of this paper attempts to construct a confidence interval for C_{pm}, which measures process variability as well as process centering in terms of the variation of the process mean from the target value. The confidence interval derived herein is based upon the posterior distribution of C_{pm} combined with the application of highest posterior density (HPD) arising from the Bayesian decision theory. The developed interval for C_{pm} is compared, via various simulation studies, with the one published in the recent literature obtained by using the classical two-sided approach implemented on the sampling distribution of C_{pm}. The experimental results demonstrate that the improvement achieved by the proposed confidence interval holds provided that the process center deviates from the target value. A Bayesian procedure for the hypothesis testing of the Taguchi process capability is also presented with several graphical analyses under a variety of assumed parameter configurations, illustrating an additional statistical merit of the new method while a process deviation from the target value occurs.

Keywords—Process capability analysis, Bayesian approach, Highest posterior density, Confidence interval

1. INTRODUCTION

The process capability analysis (PCA) is a statistical technique for quantifying process variability and analyzing the relation of this variability to production requirements and/or product specifications under circumstances where the measurements of the quality characteristic (of interest to the process engineer) taken on process operations are independent and approximately normally distributed with a fixed process mean and a constant process standard deviation. With a view to take into account quantitatively both the process variability and departure from the target value in assessing a process's capability, Chan et al. (1988) and Boyles (1991a, 1991b) separately proposed and discussed an alternative process capability index (PCI), C_{pm}, by borrowing the loss function from Taguchi's (1986) philosophies of quality engineering. Of late, the Taguchi index of this type has been receiving considerable attention in the literature (Zimmer and Hubele, 1997; Shiau et al., 1999; Deleryd and Vannman, 1999; and Zimmer et al., 2001).

There have various other measures available for industrial use when conducting PCA. Most recently, a profound literature review on the development of PCIs accompanied with a panel discussion is given in Kotz and Johnson (2002). To date, the two most widely used PCI's in common practice are C_p and C_{pk}. Sullivan (1984, 1985) and Kane (1986a, 1986b) provided comprehensive insights of these two indices into real-world applications alongside their statistical sampling properties. In Pearn, Kotz and Johnson (1992), a great deal of rigorous theoretical efforts have been devoted to the distributional developments and inferential properties of some PCI's (C_p, C_k and C_{pm}) and their estimators, as well as the so-called "third generation" PCI, C_{pmk}. Kotz and Johnson (1993) gave an overview of the grounding work recently developed for the area of process capability. Spiring (1997) suggested the use of a weight function to present a unifying approach (termed C_{pw}), allowing one to examine several statistical properties associated with estimators of the various PCI's. Capability indices are estimated through sample data, often with not very large sample sizes; thus sometimes it is of more important interest to compute interval estimators for the true capability index given a sample estimate in order to properly account for the uncertainty due to the sampling variability (see Chou et al., 1990; Kushler and Hurley, 1992; Franklin and Wasserman, 1992; Spiring, 1997; Shiau et al., 1999; and Zimmer et al., 2001;). In Spiring (1991), it has also been emphasized that C_{pm} is one of several competing indices which possess the ability to consider proximity to the target value as well as process variability when assessing process capability. For the above reasons, the main focus of this paper will be on constructing confidence limits for the Taguchi capability index C_{pm}.

In this research, a Bayesian alternative for C_{pm} to the existing methods presented by Boyles (1991) and Zimmer et al. (2001) is derived and its relative performance as compared to the classical sampling theory approaches is

* Corresponding author's email: simonfan@saturn.yzu.edu.tw

also reported. Concerning the justification and advantages of the use of Bayesian statistical techniques over classical ones, associated remarks have already been stressed in Chan, Cheng and Spiring (1988, pp. 167-168), Cheng and Spiring (1989, pp. 97-98), and Shiau et al. (1999, pp. 369-370). In short, a general framework for Bayesian solutions assumes that the parameter of interest (herein a function of the process variance, which will be introduced in a later section) is probabilistic with an unknown statistical distribution. A prior distribution is taken on this parameter and then modified in light of the likelihood function in order to reflect the behavior of the relevant data collected and arrive at a posterior distribution (see, e.g., Berger (1988) and Lee (1989)). It should first be noted that all developments throughout the paper are made assuming the process under investigation is free from any assignable cause (i.e., in a state of statistical control) and the quality characteristic under study arises approximately from a normal distribution. The research motive of this paper is attributed primarily to the pioneering work of C_{pm} by Chan et al. (1988).

For clarity of presentation, the paper is organized as follows. In Section 2 a succinct review of the Taguchi index C_{pm} is given along with the statistical properties of the measure and its estimators. A Bayes-based procedure is developed in Section 3 for providing the posterior distribution related to C_{pm}, and thus a Bayesian confidence interval can effortlessly be computed by means of univariate search methods. The Newton's or secant method is employed for this purpose (see, e,g., Conte and de Boor (1980, pp. 78-79)). Section 4 presents a variety of experimental results to underscore the new approach of having better statistical performance. In Section 5, a Bayesian-based approach for the hypothesis testing of the Taguchi process capability is presented and its statistical properties demonstrated through a series of graphical illustrations are thoroughly discussed as well. Finally, we conclude the paper and consider opportunities for future research in Section 6.

2. TAGUCHI CAPABILITY INDEX, ITS ESTIMATOR AND STATISTICAL PROPERTIES

The process capability index C_{pm} espoused by Chan et al. (1988) is defined as

$$C_{pm} = \frac{\text{USL} - \text{LSL}}{6\sigma'} \tag{1}$$

where USL, LSL represent the upper and lower specification limits, respectively, and σ' denotes the squared root of the expected mean squared error (MSE) from the target value (T), expressed as

$$\sigma'^2 = E\left(X-T\right)^2 = \sigma^2 + \left(\mu - T\right)^2 \tag{2}$$

where X is a random variable associated with measurements; σ^2 and μ are the corresponding process variance and process mean for X. The parameter σ'^2 is usually unknown and can be estimated from a random sample of taking n measurements $x_1, x_2, ..., x_n$ on the quality characteristic of interest by using

$$\hat{\sigma}'^2 = \frac{\sum_{i=1}^{n}\left(x_i - T\right)^2}{n-1} \tag{3}$$

Notice that Boyles (1991, pp. 22-23), followed by Johnson (1992, p. 212) and Shiau et al. (1999, p. 371), strongly suggests using an alternative estimator

$$\tilde{\sigma}'^2 = \frac{\sum_{i=1}^{n}\left(x_i - T\right)^2}{n} = \left(\frac{n-1}{n}\right)\hat{\sigma}'^2 \tag{4}$$

and shows that $\tilde{\sigma}'^2$ is an unbiased and also the maximum likelihood estimator (MLE) of σ'^2 with smaller MSE. Nevertheless, the choice of estimator for σ'^2 would not affect the derived Bayesian credible interval, which will be discussed in Section 3. Hence the resulting estimator of C_{pm} in (1) can be written as (Chan et al. (1988, pp. 164)

$$\hat{C}_{pm} = \frac{\text{USL} - \text{LSL}}{6\hat{\sigma}'} \tag{5}$$

Assuming the measurements $x_1, x_2, ..., x_n$ to be distributed as $N(\mu, \sigma^2)$, $(n-1)\hat{\sigma}'^2 / \sigma^2$ follows a non-central chi-square distribution with n degrees of freedom and a non-centrality parameter $\lambda = n\left(\mu - T\right)^2 / \sigma^2$, and then the probability density function (pdf) of $\hat{C}_{pm}$ can be shown as

$$f\left(\hat{C}_{pm}\right) = \frac{a}{2^{\frac{n}{2}-1}\hat{C}_{pm}^{3}} \exp\left[-\frac{1}{2}\left(\frac{a}{\hat{C}_{pm}^{2}} + \lambda\right)\right] \sum_{j=0}^{\infty} \frac{\left(\frac{a}{\hat{C}_{pm}^{2}}\right)^{\frac{n}{2}+j-1} \lambda^{j}}{\Gamma\left(\frac{n}{2}+j\right) 2^{2j} j!}; \quad 0 < \hat{C}_{pm} < \infty, \tag{6}$$

where $a = C_{pm}^{2}\left(n-1\right)\left(1+\lambda/n\right)$. For further details about the mathematical proof in (6), see Chan et al. (1988, p. 174) and Zimmer et al. (2001, pp. 65-66). As can be seen from Equation (6), the shape of $f(\hat{C}_{pm})$ depends on the values of C_{pm}, n and λ. For example in Figure 1, given the actual value of $C_{pm} = 1.5$ and a fixed sample size $n = 10$ with varying λ's, it shows that the kurtosis increases as λ gets larger but the skewness tends to fall off. As such, the rising peakedness as a result of the departure of the process mean from the target value gives rough guidance about the types of processes for which a Bayesian-based confidence interval might be advantageous.

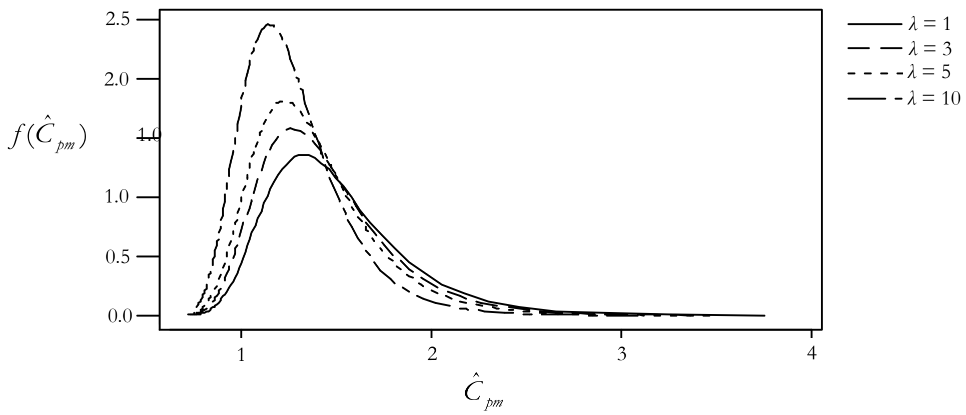

Figure 1. The probability density functions of $\hat{C}_{pm}$ for various non-centrality parameters λ = 1, 3, 5, 10 when C_{pm} = 1.5 and n=10.

According to the pdf of $f(\hat{C}_{pm})$, its expected value and variance can exactly be found (see Chan et al. (1988, p. 174) and Pearn et al. (1992, pp. 218-220)), yet unfortunately, the statistical properties of $\hat{C}_{pm}$ involving the non-central chi-square distribution are very difficult to deal with by nature. Under a restricted case of $\mu = T$ where the indices C_p and C_{pm} are essentially equivalent, Chan et al. (1988) recommended two analytical procedures to examining $\hat{C}_{pm}$—an operating characteristic (OC) curve approach and a Bayesian-type approach. The OC curve approach is built upon the traditional frequentist theory to investigate the sampling distribution of $\hat{C}_{pm}$; however, this approach will produce pragmatic unwieldiness while evaluating the stochastic properties of $\hat{C}_{pm}$. In contrast, the Bayesian approach, akin to the one for C_p posed in Cheng and Spiring (1989), can find exact (and/or approximate) credible intervals for C_{pm} that are much easier to interpret for a general purpose and less restrictive than those generated by using the OC curve approach. Following Chan et al.'s (1988) work, Shiau et al. (1999) employed a multi-parameter joint prior (for μ and σ) and provided a general Bayesian procedure for assessing the process capability index C_{pm} without relying on the assumption that $\mu = T$. The section that follows will proceed to the development of a modified Bayesian approach where a suitable reference prior about the process variance is opted and a closed-form expression of numerical integral is derived to cope with the general situations frequently found to occur in ordinary QC practice; that is, the process mean μ is not on the target value T.

3. A GENERALIZED BAYESIAN APPROACH FOR ANALYZING C_{pm}

3.1 Prior distribution

Assume that the process measurements of the quality characteristic conform to a normal distribution $N(\mu,\ \sigma^2)$, and then due to their independency and being identically distributed (i.i.d.), the likelihood function for the random sample $X = \{x_1,\ x_2,\ ...,\ x_n\}$ will be

$$L(\sigma^2 | X) \propto (\sigma^2)^{-\frac{n}{2}} \exp\left[-\frac{\sum_{i=1}^{n}(x_i - \mu)^2}{2\sigma^2} \right] \tag{7}$$

where the process variance σ^2 is our key interest and assumed stochastic with an associated statistical distribution. The general argument is that Bayesian inferences about variances are usually more important concerns than those about means if the underlying distribution turns out to be only approximately normal (Lee, 1989). To begin with the construction of a Bayesian approach for analyzing C_{pm}, we must decide on an appropriate prior for the unknown parameter σ^2. When there is no obvious prior information on hand, the justification of a particular prior must solely rest on the sampling distribution since it is the only available information (see, e.g., Berger (1988) and Robert (1994)). Therefore, the Jeffreys' noninformative prior distribution depending on Fisher's information is considered here in the form

$$\pi(\sigma^2) \propto \frac{1}{\sigma^2} \tag{8}$$

where π denotes the prior distribution and for a detailed account regarding the above relation, see Berger (1988) and

APPENDIX A. The prior as shown in (8) is improper; however, it will turn out that the prior distribution can combine with an ordinary likelihood to give a posterior which is proper. It is worth while to note that the prior provided by Jeffreys' rule actually satisfies the *invariant reparameterization requirement* that whatever scale is chosen to measure the unknown parameter, the same prior results hold as the scale is transformed to any particular scale. This seems a highly valuable property for a reference prior.

3.2 Posterior distribution

Combining the prior $\pi(\sigma^2)$ based on the amount of information brought by an experiment (or the observations) about σ^2 with the likelihood function as in (7), the posterior of σ^2 is (see APPENDIX B)

$$\pi\left(\sigma^2|X\right) = \frac{1}{\Gamma\left(\frac{n}{2}\right)}\left(\frac{(n-1)\hat{\sigma}^2+n(\bar{x}-\mu)^2}{2}\right)^{\frac{n}{2}}\left(\sigma^2\right)^{-\left(\frac{n}{2}+1\right)} \times\exp\left[-\frac{(n-1)\hat{\sigma}^2+n(\bar{x}-\mu)^2}{2\sigma^2}\right]; 0\le\sigma^2\le\infty, \tag{9}$$

where $\hat{\sigma}^2=\sum_{i=1}^{n}(x_i-\bar{x})^2/(n-1)$. Because $\sigma'^2=\sigma^2+(\mu-T)^2$, the posterior distribution of σ' can be obtained as follows

$$\pi\left(\sigma'|X\right)=\frac{2\sigma'}{\Gamma\left(\frac{n}{2}\right)}\left(\frac{(n-1)\hat{\sigma}^2+n(\bar{x}-\mu)^2}{2}\right)^{\frac{n}{2}}\times \left[\sigma'^2-(\mu-T)^2\right]^{-\left(\frac{n}{2}+1\right)}\exp\left[-\frac{(n-1)\hat{\sigma}^2+n(\bar{x}-\mu)^2}{2\left[\sigma'^2-(\mu-T)^2\right]}\right]; \sqrt{(\mu-T)^2}\le\sigma'\le\infty \tag{10}$$

Consequently, the posterior probability of C_{pm} lying inside the interval $[\varpi,\ \omega]$ is

$$\begin{aligned}
p &= \Pr\left[\varpi\le C_{pm}\le\omega|X\right]=\Pr\left[\varpi\le\frac{\text{USL}-\text{LSL}}{6\sigma'}\le\omega|X\right]\\
&=\Pr\left[\frac{\text{USL}-\text{LSL}}{6\omega}\le\sigma'\le\frac{\text{USL}-\text{LSL}}{6\varpi}|X\right]\\
&=\int_{h_1}^{h_2}\pi\left(\sigma'|X\right)d\sigma'\\
&=\int_{h_1}^{h_2}\left[\frac{2\sigma'}{\Gamma\left(\frac{n}{2}\right)}\right]\left[\frac{(n-1)\hat{\sigma}^2+n(\bar{x}-\mu)^2}{2}\right]^{\frac{n}{2}} \times\left[\sigma'^2-(\mu-T)^2\right]^{-\left(\frac{n}{2}+1\right)} \times\exp\left[-\frac{(n-1)\hat{\sigma}^2+n(\bar{x}-\mu)^2}{2\left[\sigma'^2-(\mu-T)^2\right]}\right]d\sigma'\\
&=\int_{k_1}^{k_2}\frac{1}{\Gamma\left(\frac{n}{2}\right)}y^{\frac{n}{2}-1}e^{-y}dy,
\end{aligned} \tag{11}$$

where

$h_1=(\text{USL}-\text{LSL})/6\omega$, $h_2=(\text{USL}-\text{LSL})/6\varpi$

$y=[(n-1)\hat{\sigma}^2+n(\bar{x}-\mu)^2]/2[\sigma'^2-(\mu-T)^2]$

$k_1=[(n-1)\hat{\sigma}^2+n(\bar{x}-\mu)^2]/2[(\hat{\sigma}'^2/\varpi^2)\hat{C}_{pm}^2-(\mu-T)^2]$

and

$k_2=[(n-1)\hat{\sigma}^2+n(\bar{x}-\mu)^2]/2[(\hat{\sigma}'^2/\omega^2)\hat{C}_{pm}^2-(\mu-T)^2]$

To construct a $100p\%$ two-sided Bayesian credible interval $[\varpi,\ \omega]$ for C_{pm}, it is first required to calculate the values of k_1 and k_2 corresponding to desirable credibility p. It is then easy to verify that the Bayesian interval limits for C_{pm} are

$$\varpi=\sqrt{\frac{2k_1\hat{\sigma}'^2\hat{C}_{pm}^2}{\left[(n-1)\hat{\sigma}^2+n(\bar{x}-\mu)^2+2k_1(\mu-T)^2\right]}},\quad \omega=\sqrt{\frac{2k_2\hat{\sigma}'^2\hat{C}_{pm}^2}{\left[(n-1)\hat{\sigma}^2+n(\bar{x}-\mu)^2+2k_2(\mu-T)^2\right]}}. \tag{12}$$

It is obviously to see from Equation (12) that the Bayesian interval for C_{pm} is invariant to any kind of point estimators of σ'^2 used to provide a point estimator of C_{pm}. The resultant form of posterior in (11) obeys $Gamma(n/2,\ 1)$. The knowledge of the posterior distribution allows for the derivation of confidence regions, via highest posterior density (HPD) regions, as will be described shortly.

3.3 Computation of highest posterior density (HPD) region

Unlike classical confidence intervals that can only be interpreted in terms of "coverage probability" in a long-run sampling sense, Bayesian credible intervals are directly referred to the probability of the unknown parameter being in a pre-assigned interval given the data observed in the current experiment since, meaningfully speaking, the posterior distribution is an actual pdf of the parameter. We often use the notion of *highest posterior density* (HPD) to determine an appropriate credible interval. As with choosing a credible interval, it is typically desired to try to minimize its size. To achieve this, one should contain only those points (in a set) that have the largest posterior density, namely the "most likely" values of the unknown parameter. The HPD credible set is defined below (see

Berger (1988)).

Definition 1. For a prior distribution $\pi(\theta)$ and a posterior distribution $\pi(\theta|X)$ of θ, a set C_x is termed an *a-credible set* if

$$P^{\pi(\theta|X)}(\theta \in C_x|X) \geq 1-\alpha$$

Definition 2. The $100(1-\alpha)\%$ *HPD credible set* for θ is of the form

$$C_x^\alpha = \{\theta : \pi(\theta|X) \geq k_\alpha\}$$

where k_α is the largest bound such that

$$P^{\pi(\theta|X)}\left(\theta \in C_x^\alpha|X\right) \geq 1-\alpha$$

An application of HPD regions to this research is motivated mainly by the fact that they are "continuous" and minimize specifically the volume of the credible set provided that the posterior density is unimodal. The concept of HPD credible set is roughly sketched in Figure 2.

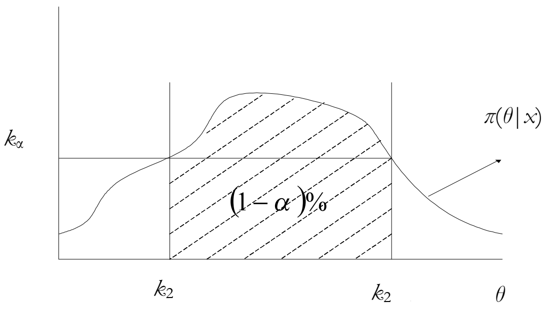

Figure 2. The highest posterior density (HPD) credible set.

Indeed, the posterior distribution of C_{pm} is unimodal and asymmetric, so equating the two tail probabilities, as normally done by classical statistics, is clearly not an optimal answer for this case. HPD regions are not in general equal tailed. On that account, we propose utilizing the Newton's or secant method (see, e.g., Conte and de Boor (1980, pp. 78-79)) to solve the nonlinear equation

$$\pi(y|X) - k_\alpha = \frac{1}{\Gamma\left(\frac{n}{2}\right)} y^{\frac{n}{2}-1} e^{-y} - k_\alpha = 0 \tag{13}$$

where k_α is an initial guess, for k_1 and k_2 that form the HPD region for the intermediate parameter y. If the initial guess of k_α yields the posterior probability short of $(1-\alpha)$, then it indicates that the highest density lower bound k_α is set too high and should be lowered; otherwise, it should be raised. Until a set of (k_1, k_2) with respect to a specific value of k_α is positioned such that the computed posterior probability p in (11) approximately equals $100(1-\alpha)\%$ as specified beforehand. Thus, the HPD credible interval $[\varpi, \omega]$ for C_{pm} can readily be located in terms of Equation (12). It turns out to be surprisingly simple from our earlier experience to carry out the univariate search procedures for the root-seeking problem (as mentioned previously) in a spreadsheet application. For an algorithmic presentation, the searching procedure is summarized in the following.

Algorithm 1. (HPD Searching Procedure)

Initialization. Choose an initial value $0 < k_\alpha^0 < (n/2-1)$ in that for $Gamma(a,b)$ with $a>1$ the maximum value of the density occurs at the point $(a-1)b$. Set the upper bound $U := (a-1)b$ and the lower bound $L := 0$ for k_α. Set $j := 0$ and choose a tolerance $\delta > 0$ (say, 1×10^{-6}) for halting the algorithm. Given an a level.

Step 1. Solve the nonlinear equation

$$\frac{1}{\Gamma\left(\frac{n}{2}\right)} y^{\frac{n}{2}-1} e^{-y} - k_\alpha^j = 0 \tag{14}$$

by using the Newton's method (with derivative) or the secant method (without derivative). Denote the incumbent solution as $C_x^\alpha := (k_1, k_2)$. Notice that each pair of roots for Equation (14) can be found without undue difficulty if the starting point employed is defaulted to zero for searching k_1 and a larger value (say, 10) for searching k_2.

Step 2. Calculate the probability

$$P(C_x^\alpha) = \int_{k_1}^{k_2} \frac{1}{\Gamma\left(\frac{n}{2}\right)} y^{\frac{n}{2}-1} e^{-y} dy$$

Step 3. If $\left|P(C_x^\alpha) - (1-\alpha)\right| \leq \delta$, then stop and return the solution $C_x^\alpha = (k_1, k_2)$; otherwise go to Step 4.

Step 4. If $P(C_x^\alpha) > (1-\alpha)$, then update k_α's lower bound by $L := k_\alpha^j$, set $k_\alpha^{j+1} := (k_\alpha^j + U)/2$ and $j := j+1$, and go to Step 1.

Step 5. If $P(C_x^\alpha) < (1-\alpha)$, then update k_α's upper bound by $U := k_\alpha^j$, set $k_\alpha^{j+1} := (k_\alpha^j + L)/2$ and $j := j+1$, and go to Step 1.

In the preceding algorithm, the bisection method is employed for the outer loop to solve the nonlinear equation

$$P(C_x^{\alpha})-(1-\alpha)=\int_{k_1}^{k_2}\frac{1}{\Gamma\left(\frac{n}{2}\right)}y^{\frac{n}{2}-1}e^{-y}dy-(1-\alpha)=0 \qquad (15)$$

which is a convex and monotone decreasing function. Algorithm 1 is only a crude but effective implementation, and a more efficient bracketing procedure, such as the method of modified regula falsi (see, e.g., Conte and de Boor (1980)), may be used instead. To be illustrated next are some interesting experimental results of the proposed HPD credible interval for C_{pm} based on a wide variety of simulations as compared to those of an analog by using classical sampling statistics.

4. PERFORMANCE OF AN HPD CREDIBLE INTERVAL FOR C_{pm}

We now analyze the comparative performance of the Bayesian HPD credible interval addressed in Section 3. The whole comparison report is divided into two subsequent scenarios. To avoid ambiguity, henceforth the "confidence interval" refers to the interval estimator founded on the classical sampling distribution and the "credible interval" relates to the interval estimator based upon the Bayesian posterior distribution.

4.1 The equal-tailed confidence interval versus the HPD credible interval when $\mu = T$

The condition that $\mu = T$ indicates $\lambda = 0$ in the sampling distribution of $\hat{C}_{pm}$ as exhibited in Equation (6). Adapting Zimmer et al.'s (2001, p. 52) two-sided $100(1-\alpha)\%$ confidence interval on C_{pm} with $\lambda = 0$ to the point estimator of $\hat{\sigma}'^2$ defined in (3) yields

$$\frac{\hat{C}_{pm}}{\sqrt{\dfrac{n-1}{\chi^2_{\frac{\alpha}{2};n}}}}\le C_{pm}\le\frac{\hat{C}_{pm}}{\sqrt{\dfrac{n-1}{\chi^2_{1-\frac{\alpha}{2};n}}}} \qquad (16)$$

where χ^2_n follows a "central" chi-square distribution with n degrees of freedom. In fact, the above confidence interval depends only on the value of $\hat{C}_{pm}$ and the sample size n. The confidence length R_1 of Equation (16) is defined as

$$R_1=\frac{\hat{C}_{pm}}{\sqrt{\dfrac{n-1}{\chi^2_{1-\frac{\alpha}{2};n}}}}-\frac{\hat{C}_{pm}}{\sqrt{\dfrac{n-1}{\chi^2_{\frac{\alpha}{2};n}}}} \qquad (17)$$

Consider also a two-sided $100(1-\alpha)\%$ HPD credible interval of C_{pm} when $\mu = T$. During Step 1 of Algorithm 1, the Newton's method is selected for use to look for the roots (k_1', k_2') inasmuch as the derivative of Equation (13) is accessible. Consequently, the HPD credible interval limits for C_{pm} are reduced to

$$\varpi'=\sqrt{2k_1'\hat{C}^2_{pm}\big/(n-1)}$$
$$\omega'=\sqrt{2k_2'\hat{C}^2_{pm}\big/(n-1)}\ , \qquad (18)$$

and the credibility length R_2 is defined by

$$R_2=\sqrt{2k_2'\hat{C}^2_{pm}\big/(n-1)}-\sqrt{2k_1'\hat{C}^2_{pm}\big/(n-1)}\ . \qquad (19)$$

Likewise, the above HPD credible interval depends only on the value of $\hat{C}_{pm}$ and the sample size n.

To compare these two types of interval estimators presented in (16) and (18) for the situation where $\mu = T$, suppose that $\hat{C}_{pm}=1.3$ (resulting from the process being very likely capable) and $1-\alpha=0.95$, and then we compute the performance measure given by

$$P_1=(R_2-R_1)/R_2\times 100\%, \qquad (20)$$

the improving percentage of the confidence interval in (16) relative to the HPD credible interval in (18). [It is noteworthy that Juran et al. (1979) ever suggested a minimum value of the process potential, $C_p = 1.33$, generally used for an ongoing process.] The numerical results of P1 corresponding to various sample sizes from $n=3$ to $n = 100$ are listed in Table 1.

As can apparently be seen from Table 1, while assessing the process capability by means of building an interval estimate on the Taguchi index C_{pm} for the case where $\mu = T$ and $\alpha = 0.05$, the two-sided classical confidence interval is always slightly shorter than the two-sided Bayesian credible interval. Whilst the sample size n becomes larger, the improving percentage P_1 diminishes, ranging from 5.50% to 0.19% in the scale of R_2. To be more precisely, the maximum length difference between R_1 and R_2 is merely 0.134529 occurring at $n=3$.

To gain a better understanding of the interval estimates' location, Figure 3 plots the upper and lower limits for both interval estimates of C_{pm} from $n=3$ to $n=100$ using the same data as computed in Table 1. It reveals that, in essence, the two interval estimators are virtually identical and asymptotically approaching each other for larger samples. In this instance where $\mu = T$, these two intervals are nearly symmetric to the center line of point estimate ($\hat{C}_{pm}=1.3$) and noticeably reduced to the right as more observational data is collected.

Table 1. The improving percentage of the confidence interval in (16) relative to the credible interval in (18) when $1-\alpha$ = 0.95 and $\mu = T$

n	p_2	n	p_2	n	p_2	n	p_2	n	p_2	n	p_2
3	5.342519	21	1.085549	39	0.570050	57	0.354072	75	0.295128	93	0.213715
4	5.501611	22	1.000491	40	0.538438	58	0.380519	76	0.278976	94	0.208100
5	4.647851	23	0.989305	41	0.559535	59	0.366341	77	0.269158	95	0.224764
6	3.931649	24	0.932785	42	0.553114	60	0.357462	78	0.290116	96	0.212275
7	3.355450	25	0.897576	43	0.538415	61	0.367048	79	0.258988	97	0.188890
8	2.917394	26	0.867604	44	0.535350	62	0.321048	80	0.275545	98	0.216711
9	2.594895	27	0.837334	45	0.522166	63	0.365454	81	0.261834	99	0.215726
10	2.338870	28	0.788154	46	0.477852	64	0.329700	82	0.268382	100	0.191907
11	2.129601	29	0.764841	47	0.485100	65	0.347591	83	0.277350		
12	1.914338	30	0.784795	48	0.479777	66	0.320674	84	0.261493		
13	1.752642	31	0.727864	49	0.462065	67	0.323536	85	0.247999		
14	1.638307	32	0.692420	50	0.431223	68	0.305753	86	0.251623		
15	1.505809	33	0.693290	51	0.429865	69	0.317103	87	0.223902		
16	1.439206	34	0.662417	52	0.436857	70	0.307731	88	0.235801		
17	1.350390	35	0.630559	53	0.417910	71	0.328346	89	0.241548		
18	1.251091	36	0.624464	54	0.384025	72	0.274023	90	0.214836		
19	1.207011	37	0.616433	55	0.390382	73	0.302465	91	0.226040		
20	1.144950	38	0.576549	56	0.399427	74	0.282564	92	0.236573		

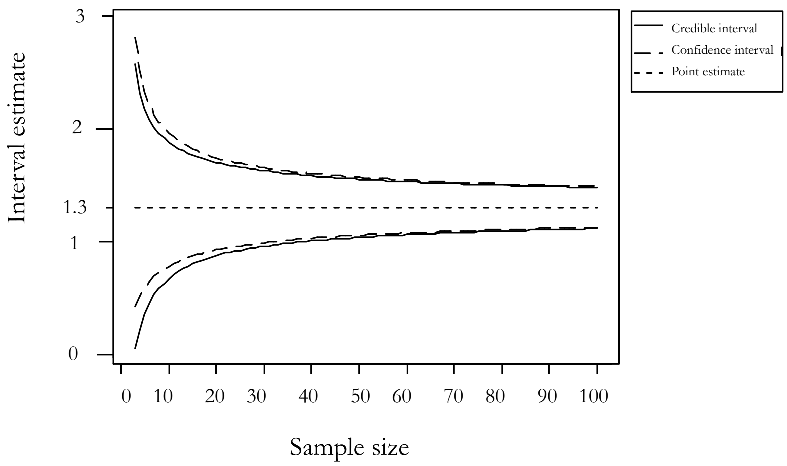

Figure 3. The 95% two-sided confidence and HPD credible intervals for C_{pm} when $\hat{C}_{pm} = 1.3$ and $\mu = T$ $(n = 3,\ 4,\ \ldots,\ 100)$.

4.2 The equal-tailed confidence interval versus the HPD credible interval when $\mu \neq T$

When $\mu = T$ (which is a more realistic circumstance for regular QC practice) and if the point estimator $\hat{\sigma}'^2$ in (3) is utilized instead of $\tilde{\sigma}'^2$ in (4), Zimmer, Hubele and Zimmer's (2001, p. 52) two-sided $100(1-\alpha)\%$ confidence interval for C_{pm} becomes

$$\frac{\hat{C}_{pm}}{\sqrt{1+\frac{\lambda}{n}}\sqrt{\frac{n-1}{\chi^2_{\frac{\alpha}{2};n,\lambda}}}} \le C_{pm} \le \frac{\hat{C}_{pm}}{\sqrt{1+\frac{\lambda}{n}}\sqrt{\frac{n-1}{\chi^2_{1-\frac{\alpha}{2};n,\lambda}}}} \qquad (21)$$

where $\chi^2_{n,\lambda}$ obeys a non-central chi-square distribution with n degrees of freedom and a non-centrality parameter λ. The confidence interval for the case of $\mu \neq T$ depends on the value of $\hat{C}_{pm}$, the sample size n and the non-centrality parameter λ. It is of great importance to note from Equation (21) that, regardless of the location of process mean (i.e., $\mu = T$ or $\mu \neq T$), the confidence intervals for C_{pm} as demonstrated in Equations (16) and (21) are invariant to the employment of different point estimators of σ'^2 as well, such as $\hat{\sigma}'^2$ and $\tilde{\sigma}'^2$. The confidence length R_3 of Equation (21) is given by

$$R_3 = \frac{\hat{C}_{pm}}{\sqrt{1+\frac{\lambda}{n}}\sqrt{\frac{n-1}{\chi^2_{1-\frac{\alpha}{2};n,\lambda}}}} - \frac{\hat{C}_{pm}}{\sqrt{1+\frac{\lambda}{n}}\sqrt{\frac{n-1}{\chi^2_{\frac{\alpha}{2};n,\lambda}}}} \qquad (22)$$

IJOR Vol. 3, No. 1, 56–75 (2006)

Again, consider a two-sided $100(1-\alpha)\%$ HPD credible interval on C_{pm} when $\mu \neq T$. For this situation, Algorithm 1 is applied to searching for the roots (k_1, k_2) in Equation (12) and then the credibility length R_4 is defined by $R_4 = \omega - \varpi$.

To compare the confidence interval in (21) and the HPD credible interval in (12) for the case that $\mu \neq T$, assume that $\mathrm{USL} = 125$, $\mathrm{LSL} = 75$, $\alpha = 0.05$ and the process measurements taken are approximately distributed as $N(100,\ 5)$; define the performance measure given by

$$P_2 = \left(R_3 - R_4\right)/R_3 \times 100\% \tag{23}$$

the improving percentage of the HPD credible interval in (12) relative to the confidence interval in (21). The scale of deviations from the target value is dictated by the non-centrality parameter λ. The experimental results of P_2, created from single sampling data, for various sample sizes ($n = 5,\ 10,\ 20,\ \ldots,\ 100$) and deviations from the target value ($\lambda = 1,\ 2,\ \ldots,\ 10$) are exhibited in Table 2.

Table 2. The improving percentage of the credible interval in (12) relative to the confidence interval in (21) when $1-\alpha$ = 0.95 and $\mu \neq T$

	$n=5$	$n=10$	$n=20$	$n=30$	$n=40$	$n=50$	$n=60$	$n=70$	$n=80$	$n=90$	$n=100$
$\lambda=1$	**-4.2424**	1.0309	6.9336	**-2.4890**	4.3422	1.5337	0.7505	0.0842	0.3547	**-0.2462**	2.0906
$\lambda=2$	1.6818	8.7962	12.8417	**-2.0789**	7.8879	3.3180	1.9524	1.0470	1.2454	0.4319	3.6394
$\lambda=3$	5.7395	15.1368	17.6896	**-1.4033**	10.9883	4.9917	3.1236	2.0669	2.1514	1.2045	5.0299
$\lambda=4$	8.5747	20.2879	21.7774	**-0.6332**	13.7670	6.5698	4.2557	3.0957	3.0502	2.0123	6.3208
$\lambda=5$	10.6248	24.5451	25.2879	0.1706	16.2882	8.0624	5.3473	4.1159	3.9341	2.8328	7.5364
$\lambda=6$	12.1548	28.1292	28.3457	0.9806	18.5944	9.4777	6.3994	5.1194	4.7997	3.6548	8.6904
$\lambda=7$	13.3305	31.1971	31.0401	1.7828	20.7169	10.8224	7.4134	6.1024	5.6457	4.4720	9.7914
$\lambda=8$	14.2596	33.8610	33.4375	2.5703	22.6801	12.1025	8.3912	7.0628	6.4716	5.2807	10.8456
$\lambda=9$	15.0136	36.2028	35.5885	3.3393	24.5035	13.3231	9.3345	7.9997	7.2773	6.0785	11.8578
$\lambda=10$	15.6416	38.2835	37.5324	4.0880	26.2031	14.4889	10.2452	8.9129	8.0631	6.8640	12.8318

	$n=5$	$n=10$	$n=20$	$n=30$	$n=40$	$n=50$	$n=60$	$n=70$	$n=80$	$n=90$	$n=100$
$\lambda=1$	**-4.2424**	1.0309	6.9336	**-2.4890**	4.3422	1.5337	0.7505	0.0842	0.3547	**-0.2462**	2.0906
$\lambda=2$	1.6818	8.7962	12.8417	**-2.0789**	7.8879	3.3180	1.9524	1.0470	1.2454	0.4319	3.6394
$\lambda=3$	5.7395	15.1368	17.6896	**-1.4033**	10.9883	4.9917	3.1236	2.0669	2.1514	1.2045	5.0299
$\lambda=4$	8.5747	20.2879	21.7774	**-0.6332**	13.7670	6.5698	4.2557	3.0957	3.0502	2.0123	6.3208
$\lambda=5$	10.6248	24.5451	25.2879	0.1706	16.2882	8.0624	5.3473	4.1159	3.9341	2.8328	7.5364
$\lambda=6$	12.1548	28.1292	28.3457	0.9806	18.5944	9.4777	6.3994	5.1194	4.7997	3.6548	8.6904
$\lambda=7$	13.3305	31.1971	31.0401	1.7828	20.7169	10.8224	7.4134	6.1024	5.6457	4.4720	9.7914
$\lambda=8$	14.2596	33.8610	33.4375	2.5703	22.6801	12.1025	8.3912	7.0628	6.4716	5.2807	10.8456
$\lambda=9$	15.0136	36.2028	35.5885	3.3393	24.5035	13.3231	9.3345	7.9997	7.2773	6.0785	11.8578
$\lambda=10$	15.6416	38.2835	37.5324	4.0880	26.2031	14.4889	10.2452	8.9129	8.0631	6.8640	12.8318

Evidently from Table 2, when investigating the process capability by means of constructing an interval estimate on the Taguchi index C_{pm} for the case where $\mu \neq T$ and $\alpha = 0.05$, the two-sided Bayesian credible interval is considerably shorter than the two-sided classical confidence interval, except six unpredicted instances indicated by a negative value in Table 2. The improving percentage P_2 decreases as the sample size n gets larger, but increases as more serious departures of the process mean from the target value take place. To attain to more precision results, nine additional samplings are performed and the "averaged" improving percentages, $\overline{P}_2 = \sum_{i=1}^{10} P_{2i}/10$, are reported in Table 3.

It is probably manifest that when $\mu \neq T$ the credible interval generated by using the Bayesian HPD approach outclasses the classical confidence interval at the interval length in that no negative entry appears in Table 3. Current industry practice tends to favor smaller samples in the stage of control charting, particularly in high-volume manufacturing processes (Montgomery (2001)). The sample sizes $n \leq 20$ are typically chosen for economical usage in designing a variable control chart, in which cases the value of $\overline{P}_2$ varies from 2.97% to 37.71% in the scale of R_3. In the extreme case with $\overline{P}_2 \approx 37\%$ when $n = 5$ and $\lambda = 10$, the target value T is sited at a position about 1.414 standard deviations away from the process mean, viz. $T = \mu \pm \sigma\sqrt{\lambda / n}$, which should still be within the specification limits in normal practice. Nonetheless, much effort must additionally be made on account of adjustments necessary by these departures from the target value.

In order to pictorially reflect the differentiation between the HPD credible and classical confidence intervals for the situations where $\mu \neq T$, the interval limits of these two interval estimates for $n = 5,\ 10,\ 20$ through the same data illustrated in Table 2 are sketched in Figures 4-6.

Table 3. The averaged improving percentage of the credible interval in (12) relative to the confidence interval in (21) when $1-\alpha = 0.95$ and $\mu \neq T$

	$n=5$	$n=10$	$n=20$	$n=30$	$n=40$	$n=50$	$n=60$	$n=70$	$n=80$	$n=90$	$n=100$
$\lambda=1$	15.49772	3.79589	2.97416	1.97653	1.46277	1.35634	1.28042	0.80720	0.98863	1.02188	1.10991
$\lambda=2$	23.97212	10.17758	6.89076	4.71353	3.56914	3.16216	2.77036	2.04068	2.14073	2.16285	2.17820
$\lambda=3$	28.60888	15.14189	10.31399	7.21993	5.56326	4.88083	4.17744	3.25050	3.24101	3.25644	3.18301
$\lambda=4$	31.46827	19.10780	13.32239	9.51346	7.43983	6.51145	5.51324	4.42553	4.29751	4.30939	4.14230
$\lambda=5$	33.38009	22.36242	15.98865	11.61863	9.20502	8.05870	6.78513	5.56317	5.31466	5.32542	5.06392
$\lambda=6$	34.74005	25.09374	18.37149	13.55830	10.86722	9.52829	7.99881	6.66329	6.29556	6.30728	5.95249
$\lambda=7$	35.75587	27.42873	20.51733	15.35234	12.43489	10.92587	9.15897	7.72674	7.24278	7.25719	6.81122
$\lambda=8$	36.54568	29.45600	22.46313	17.01786	13.91609	12.25677	10.26975	8.75483	8.15849	8.17707	7.64251
$\lambda=9$	37.18122	31.23931	24.23853	18.56945	15.31806	13.52593	11.33470	9.74897	9.04449	9.06858	8.44833
$\lambda=10$	37.70848	32.82574	25.86747	20.01960	16.64745	14.73785	12.35704	10.71067	9.90260	9.93327	9.23033

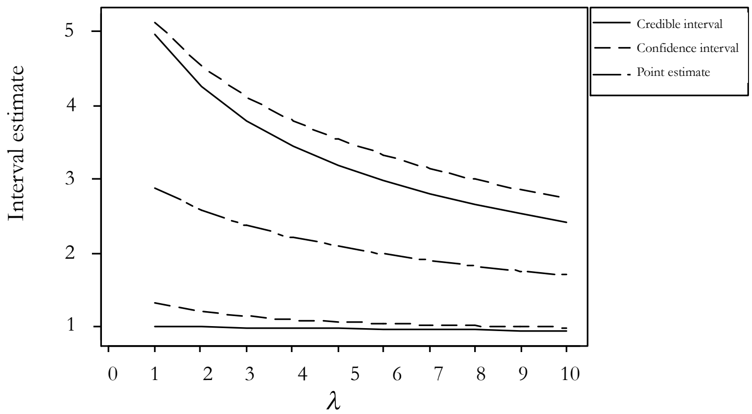

Figure 4. The 95% two-sided HPD credible and confidence intervals for C_{pm} when $n=5$ and $\mu \neq T$ ($\lambda = 1, 2, \ldots, 10$).

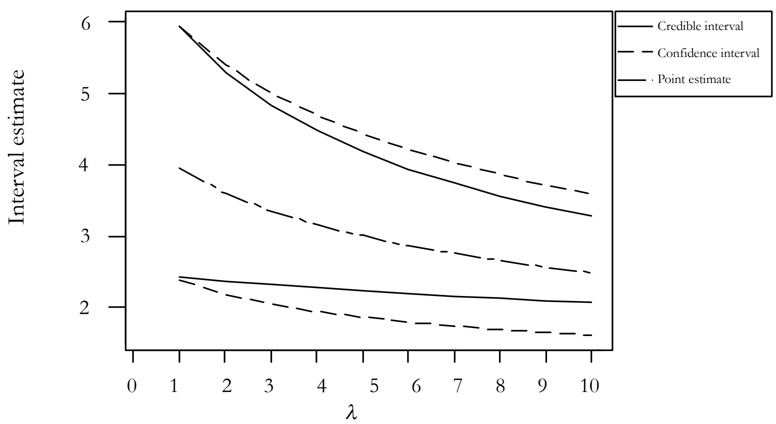

Figure 5. The 95% two-sided HPD credible and confidence intervals for C_{pm} when $n=10$ and $\mu \neq T$ ($\lambda = 1, 2, \ldots, 10$).

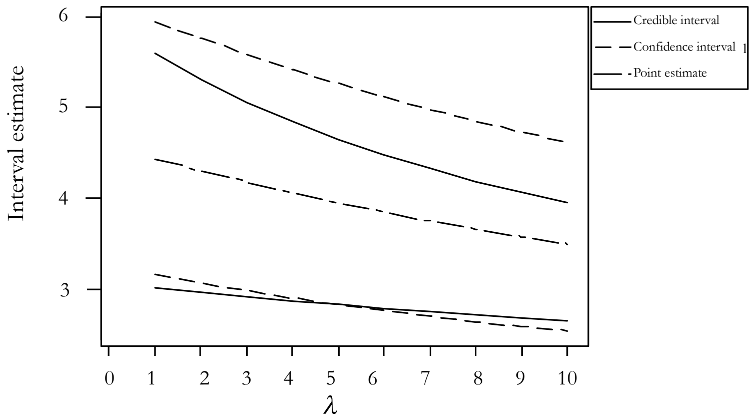

Figure 6. The 95% two-sided HPD credible and confidence intervals for C_{pm} when $n = 20$ and $\mu \neq T$ ($\lambda = 1, 2, \ldots, 10$).

In this situation, the HPD credible interval is no longer symmetric to the center line of $\hat{C}_{pm}$; both intervals decrease as the sample size n becomes larger, and also become shorter when the process mean is remote from the target value. The last statement concurs partly with the illustration in Figure 1 that the rising peakedness of $f(\hat{C}_{pm})$ due to λ will very likely render a condensed confidence interval that is shifted to the left, so does the posterior distribution of C_{pm} to which the HPD credible set is applied. Interpretatively speaking, the more widely μ is separated from T, the more assured that the process capability will definitely be getting worse, leading to a shorter and left-shifted interval estimate on C_{pm}. Since the HPD credible interval excels to a certain extent when $\mu \neq T$, it is not unreasonable to allude that the posterior distribution of C_{pm} possesses a shape with a higher kurtosis than $f(\hat{C}_{pm})$.

5. STATISTICAL PROPERTIES OF BAYESIAN HYPOTHESIS TESTING

Besides the interval estimators aforementioned, another useful tool to investigate the sampling variation of $\hat{C}_{pm}$ in (5) is to test the statistical right-tailed hypothesis:

$$\begin{aligned} &H_0 : C_{pm} \le c_0 \quad \text{(process is not capable)} \\ &H_1 : C_{pm} > c_0 \quad \text{(process is capable),} \end{aligned} \tag{24}$$

where $c_0 > 0$. In a similar manner to the test procedures posed in Kane (1986, pp. 43-44) and Chan et al. (1988, pp. 166-170), the *P*-value (or power function) of the test (24) can be computed as a yardstick to evaluate both the classical and Bayesian test statistics under a number of process configurations.

5.1 Test statistic via sampling distribution for $\mu \neq T$

Consider the hypothesis testing in (24) and the relation (see, e.g., Zimmer et al. (2001, p. 52))

$$\hat{C}_{pm} \sim C_{pm}\sqrt{1+\frac{\lambda}{n}}\sqrt{\frac{n-1}{\chi^2_{n,\lambda}}} \tag{25}$$

Therefore, the test statistic based on the sampling distribution of $\hat{C}_{pm}$ is

$$\chi^2_{n,\lambda} \sim C^2_{pm}\left(1+\frac{\lambda}{n}\right)\left(\frac{n-1}{\hat{C}^2_{pm}}\right) \tag{26}$$

In consequence of the fact that

$$C^2_{pm}\left(1+\frac{\lambda}{n}\right)\left(\frac{n-1}{\hat{C}^2_{pm}}\right) = \frac{(n-1)\hat{\sigma}'^2}{\sigma^2}, \tag{27}$$

the hypothesis test in (24) is equivalent to the left-tailed test for the process variance ($\sigma_0^2 > 0$)

$$H_0 : \sigma^2 \ge \sigma_0^2 \qquad \text{vs.} \qquad H_1 : \sigma^2 < \sigma_0^2 \tag{28}$$

giving the P-value for the test as follows

$$P\text{-}value = \Pr\left[\chi^2_{n,\lambda} \le \frac{(n-1)\hat{\sigma}'^2}{\sigma_0^2}\right] \tag{29}$$

5.2 Test statistic via posterior distribution for $\mu \neq T$

Recall that the posterior distribution is deemed as an actual pdf, so the corresponding critical region is defined as

$c = \left\{ c : C_{pm} > c_0 \right\}$ and the probability of rejecting the null hypothesis in (24) by using the posterior distribution of C_{pm} is given by

$$\alpha_1 = \Pr\left[C_{pm} > c_0 \left| X \right. \right] = \int_{c_0'}^{\infty} Gamma\left(y;\ \frac{n}{2},\ 1 \right) dy \tag{30}$$

where

$$y = \frac{(n-1)\hat{\sigma}^2 + n(\bar{x}-\mu)^2}{2\left[\sigma'^2 - (\mu - T)^2 \right]} \tag{31}$$

and

$$c_0' = \frac{(n-1)\hat{\sigma}^2 + n(\bar{x}-\mu)^2}{2\sigma_0^2} \tag{32}$$

In more detail, see APPENDIX C. The probability of failing to reject H_0 in (24) is

$$\alpha_0 = 1 - \alpha_1 = \int_0^{c_0'} Gamma\left(y;\ \frac{n}{2},\ 1 \right) dy \tag{33}$$

Note that α_0 and α_1 are a pair of test statistic used in Bayesian hypothesis testing.

5.3 Computational experience using *P*-value and α_0

For the moment, it makes sense to compare the two different types of significance probability (i.e., *P*-value and α_0) associated with the classical and Bayesian procedures as noted previously whilst conducting significance testing for the process capability index C_{pm}. A large *P*-value will cause us to favor H_0 and we should reject H_0 due to a very small *P*-value, so does α_0 in Bayesian hypothesis testing.

When $\mu = T$, the *P*-value as shown in (29) is reduced to

$$P\text{-}value = \Pr\left[\chi_n^2 \le \frac{\sum_{i=1}^{n} (x_i - \mu)^2}{\sigma_0^2} \right] \tag{34}$$

where χ_n^2 conforms to a chi-square distribution with n degrees of freedom. It can be shown that when $\mu = T$ (i.e., $\lambda = 0$) the *P*-value in (34) is exactly equivalent to α_0. See the proof in APPENDIX D, from which it is fully understood that α_0 is invariable with respect to the target value. On the contrary, the *P*-value in (29) normally varies with the non-centrality parameter λ that characterizes the locality of T. When $\mu \neq T$, the comparison results are reported under the following six process configurations.

Case I: Probability under varied target values when $\bar{x} = \mu$

Suppose that $\bar{x} = \mu = 100$, $\sigma_0^2 = 5$ and n = 5, 10, 20, 30; the *P*-value (in dash line) and α_0 (in bold-dash line) are plotted against varying target values for $\hat{\sigma}^2 = 6,\ 5,\ 4$ in Figures 7-9, respectively. Looking at these three graphs provides some following further insights into the favorable results gained from the use of the Bayesian approach addressed in this section

- The level of α_0 remains constant for each illustration in Figures 7-9.
- As the sample size n is fixed, the level of α_0 decreases in the same way as $\hat{\sigma}^2$. The reduction in $\hat{\sigma}^2$ brings about smaller values of c_0', causing α_0 to decline. The *P*-value behaves like α_0 which drops with smaller $\hat{\sigma}^2$.
- It can evidently be verified from these figures that the *P*-value and α_0 coincide only at a single point where $\mu = T$. In Figure 7 where $\hat{\sigma}^2 > \sigma_0^2$, it should be in quite more support of the null hypothesis in a sense of potential capability when the departure from the target value is negligible or not noticeable. Moreover, when the discrepancy between μ and T grows larger, α_0 is progressively greater than the *P*-value, intensely pointing out that α_0 has much more preference to $H_0 : C_{pm} \le c_0$ (or $H_0 : \sigma^2 \ge \sigma_0^2$) than the *P*-value. All the probabilities in Figure 7 fall in the range $(0.50,\ 0.76)$. The occurrence of an increasing deviation from the target value naturally lessens the process capability, so the Bayesian approach with the significance probability α_0 performs better in this situation. The larger the sample size is, the better testing performance is offered by using α_0 when the deviation from the target value is significantly present.
- In Figure 8 where the sample variance confirms the conjectured null value (i.e., $\hat{\sigma}^2 = \sigma_0^2 = 5$), the largest difference among the *P*-value and α_0 is purely around 0.05; therefore we allude that it is of little consequence to a choice between the classical and Bayesian methods for this instance.
- Figure 9 illustrates another example where $\hat{\sigma}^2 < \sigma_0^2$ and all the probabilities fall inside the range $(0.19,\ 0.50)$, implying preference to the alternative hypothesis $H_1 : C_{pm} > c_0$ (or $H_1 : \sigma^2 < \sigma_0^2$). In a word, the Bayesian procedure with α_0 will be a better alternative (having a smaller significance probability) to the hypothesis testing in case $\hat{\sigma}^2 < \sigma_0^2$ and the deviation of μ from T is negligible. For those instances where the process mean is greatly deviated from the target value, the classical test statistic ought to be adopted instead (due to its larger probability) to properly

reflect these departures from the target value in assessing the process capability.

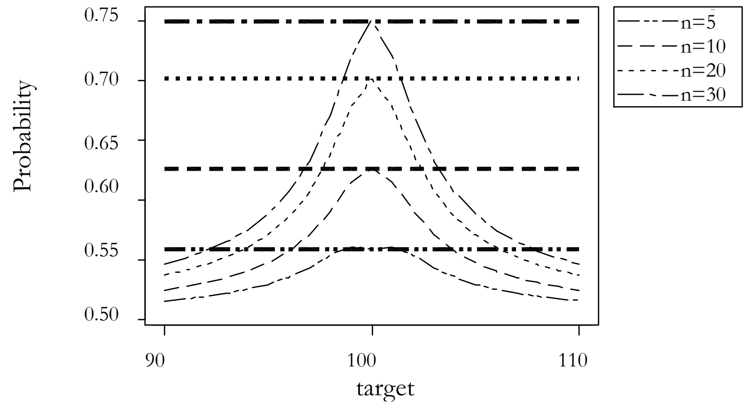

Figure 7. The *P*-value and α_0 under different target values when $\bar{x} = \mu = 100$, $\hat{\sigma}^2 = 6$, $\sigma_0^2 = 5$ and $n = 5, 10, 20, 30$.

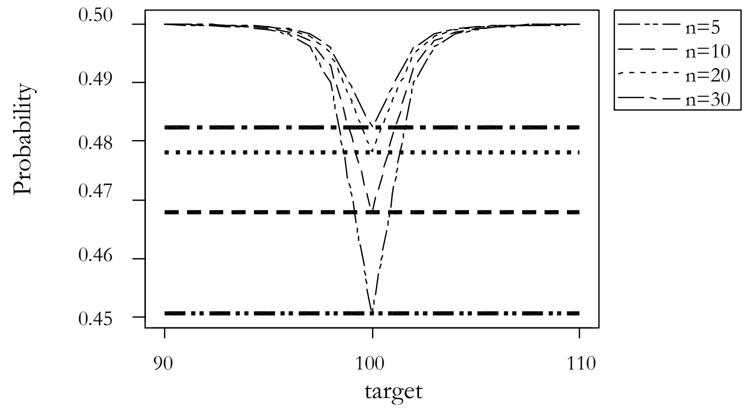

Figure 8. The *P*-value and α_0 under different target values when $\bar{x} = \mu = 100$, $\hat{\sigma}^2 = 5$, $\sigma_0^2 = 5$ and $n = 5, 10, 20, 30$.

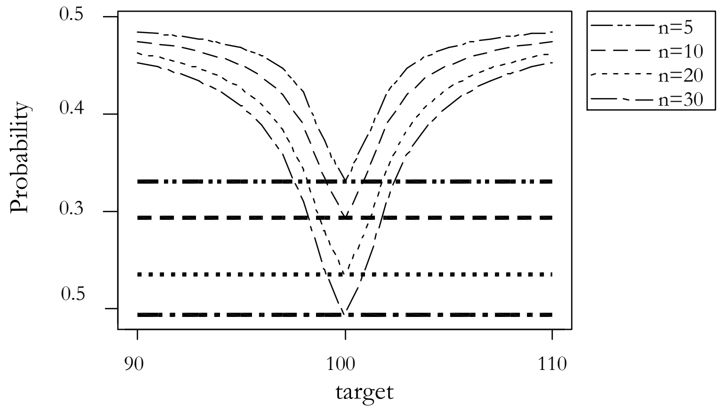

Figure 9. The *P*-value and α_0 under different target values when $\bar{x} = \mu = 100$, $\hat{\sigma}^2 = 4$, $\sigma_0^2 = 5$ and $n = 5, 10, 20, 30$.

Case II: Probability under varied target values when $\bar{x} \neq \mu$ and $\hat{\sigma}^2 = \sigma_0^2$

Assume that $\mu = 100$, $\hat{\sigma}^2 = \sigma_0^2 = 5$ and $n = 5, 10, 20, 30$; the *P*-value (in dash line) and α_0 (in bold-dash line) are plotted versus varying target values for $\bar{x}$ = 100.5, 99.5 in Figures 10-11, respectively. The analyses are outlined below.

- With the process configurations in Figures 10-11, the decision is unsettled if the deviation from the target value becomes irrelevant; that is, the target value is close to the process mean or nearby.
- When the process mean is overestimated ($\bar{x} = 100.5$) as in Figure 10 and the target value is located far right to the process mean, α_0 is increasingly greater than the *P*-value, meaning that there is a stronger tendency for α_0 to conclude $H_0 : C_{pm} \leq c_0$ than the *P*-value. Thus, the performance improvement made by the Bayesian procedure exists only if the shift on $\bar{x}$ from the process mean is incurred in the same direction as the target value. Likewise, in instances where the process mean is underestimated ($\bar{x} = 99.5$) as in Figure 11, the Bayesian approach should be a better choice as the target value is located far left to the process mean.
- It is of particular importance to note that, in situations where the Bayesian method returns an inferior result, α_0 is still kept a constant and "insensitive to the target value" level.

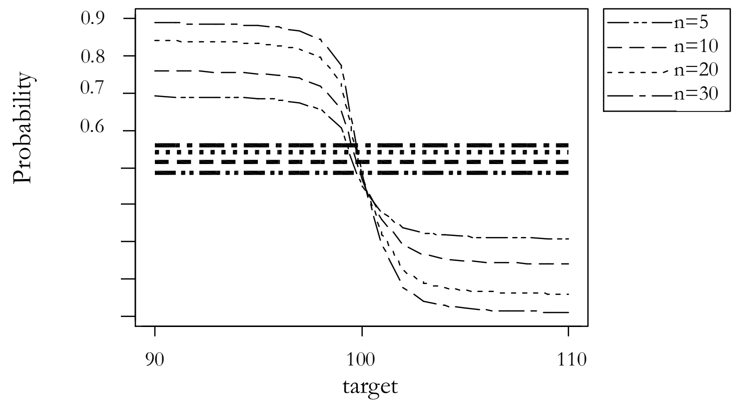

Figure 10. The P-value and α_0 under different target values when $\bar{x} = 100.5$, $\mu = 100$, $\hat{\sigma}^2 = \sigma_0^2 = 5$, and $n = 5, 10, 20, 30$.

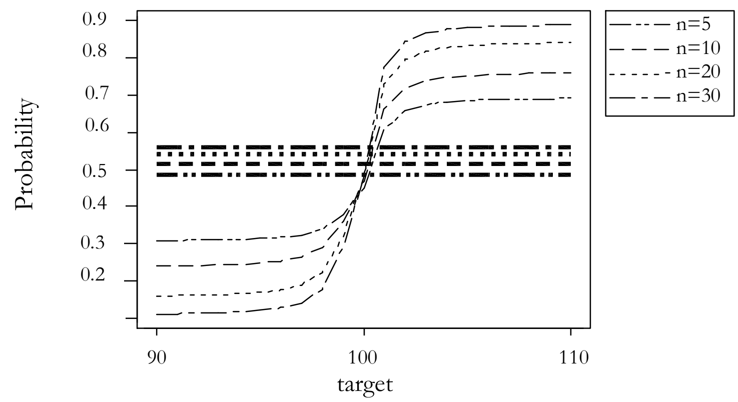

Figure 11. The P-value and α_0 under different target values when $\bar{x} = 99.5$, $\mu = 100$, $\hat{\sigma}^2 = \sigma_0^2 = 5$, and $n = 5, 10, 20, 30$.

Case III: Probability under varied sample variances when $\mu \neq T$ and $\bar{x} = \mu$

Suppose further that $\bar{x} = \mu = 100$, $T = 102$ (or 98) and $\sigma_0^2 = 5$; the *P*-value (in dash line) and α_0 (in solid line) are depicted versus varying sample variances for $n = 5, 10, 20, 30$ in Figure 12. As evidenced by these four illustrations, the Bayesian approach with α_0 shows considerable improvement (as compared to the classical test statistic) that α_0 is greater than the *P*-value when $\hat{\sigma}^2 > \sigma_0^2$, and α_0 is less than the *P*-value when $\hat{\sigma}^2 < \sigma_0^2$. This advantage gradually vanishes as the target value is approaching the process mean. According to Corollary 1, the curves of α_0 and *P*-value are joined when $\mu = T$ (Figure 12)

Case IV: Probability under varied sample variances when $\mu \neq T$ and $\bar{x} \neq \mu$

Consider the following process configurations that $\mu = 100$, $\sigma_0^2 = 5$, $T = 101$ and $n = 5, 10, 20, 30$. The *P*-value (in dash line) and α_0 (in solid line) are displayed versus varying sample variances for $\bar{x} = 100.2, 99.8$ in Figures 13-14, respectively. The computational results are reported as follows.

- When the process mean is overestimated ($\bar{x} = 100.2$) as in Figure 13 and $\hat{\sigma}^2 > 5$, α_0 is greater than the *P*-value, thus indicative of slight merit by the Bayesian procedure.
- When the process mean is underestimated ($\bar{x} = 99.8$) as in Figure 14 and $\hat{\sigma}^2 < 5$, α_0 is less than the *P*-value, suggesting a little merit of the Bayesian procedure over the classical one.
- To sum up, when the process mean is a little overestimated and $\hat{\sigma}^2 > \sigma_0^2$, the Bayesian method will be advantageous to statistical decision making of $H_0 : C_{pm} \leq c_0$; on the other hand, when the process mean is slightly underestimated and $\hat{\sigma}^2 < \sigma_0^2$, the Bayesian method will be advantageous to statistical decision making of $H_1 : C_{pm} > c_0$. (Figures 13-14)

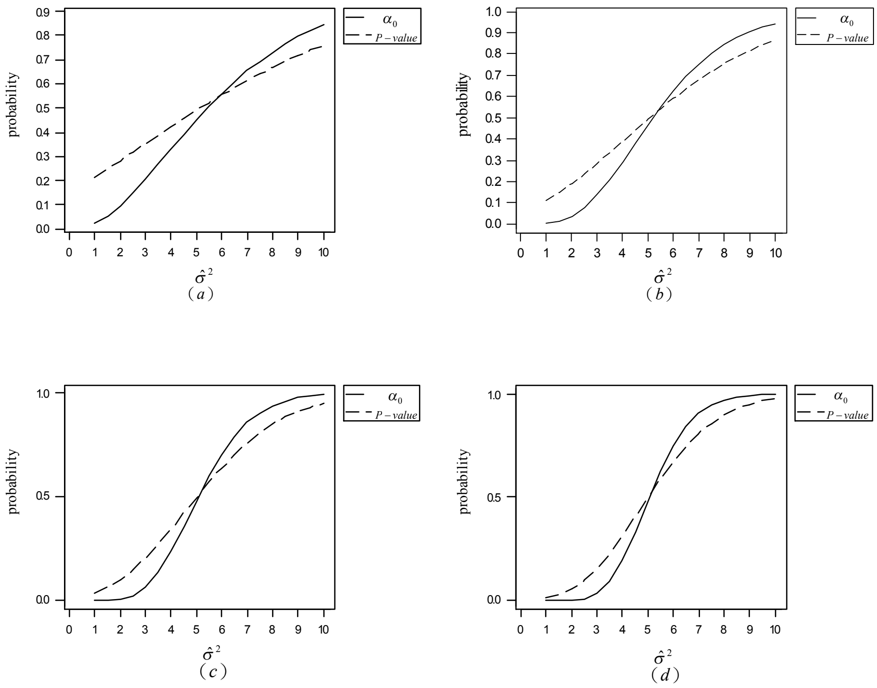

Figure 12. The *P*-value and α_0 under various sample variances when $\bar{x} = \mu = 100$, $T = 102$, $\sigma_0^2 = 5$, and (a) $n = 5$; (b) $n = 10$; (c) $n = 20$; (d) $n = 30$.

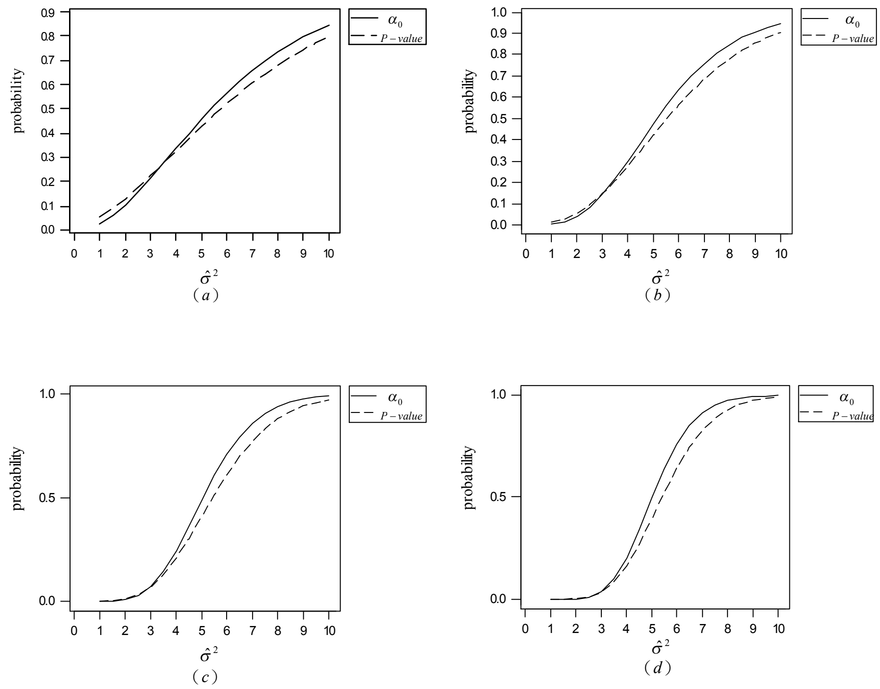

Figure 13. The *P*-value and α_0 under various sample variances when $\bar{x} = 100.2$, $\mu = 100$, $T = 101$, $\sigma_0^2 = 5$, and (a) $n = 5$; (b) $n = 10$; (c) $n = 20$; (d) $n = 30$.

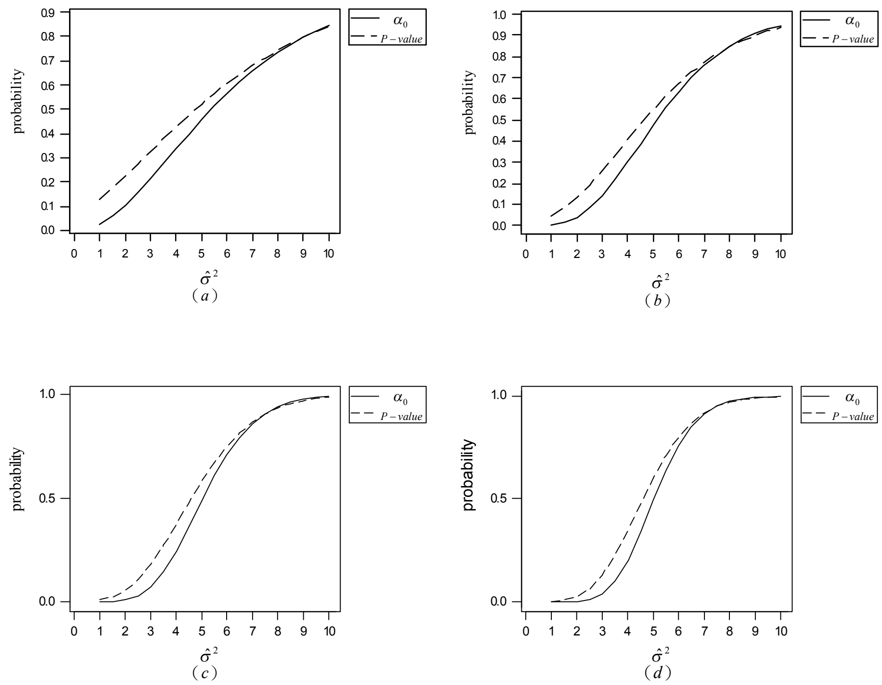

Figure 14. The *P*-value and α_0 under various sample variances when $\bar{x} = 99.8$, $\mu = 100$, $T = 101$, $\sigma_0^2 = 5$, and (a) $n = 5$; (b) $n = 10$; (c) $n = 20$; (d) $n = 30$.

Case V: Probability under varied sample means when $\mu \neq T$ and $\hat{\sigma}^2 = \sigma_0^2$

Consider the process configurations where $\mu = 100$, $\hat{\sigma}^2 = \sigma_0^2 = 5$ and $n = 5, 10, 20, 30$. The *P*-value (in dash line) and α_0 (in bold-dash line) are exhibited versus varying sample means for $T = 101,\ 99$ in Figures 15-16, respectively. As seen from Figure 15 where the departure from to the right takes place ($T = 101$), the Bayesian method has a larger significance probability to support the null hypothesis in (24) than the classical one given that the process mean is overestimated, presenting an improvement on making an adequate decision.

In contrast, when the deviation from to the left occurs ($T = 99$) as shown in Figure 16, the Bayesian method takes an advantage of a larger significance probability to favor the null hypothesis on condition that the process mean is underestimated. For this situation, it is beneficial to choose the Bayesian procedure only when the shift on the target value from the process mean is in the same way as the sample mean. If the deviation from the process mean is aggravated, the Bayesian method remains a preferable alternative. It is worth noting that the *P*-value turns out to be zero while the deviation from the process mean exceeds 3.0.

Case VI: Probability under varied sample means when $\mu \neq T$ and $\hat{\sigma}^2 \neq \sigma_0^2$

At last, suppose that $\mu = 100$, $\sigma_0^2 = 5$ and $T = 101$; the *P*-value (in dash line) and α_0 (in bold-dash line) are shown against varying sample means for $\hat{\sigma}^2 = 6,\ 4$ in Figures 17-18, respectively. It can clearly be seen from these two illustrations that the Bayesian approach shows substantial improvement with a larger significance probability (as compared to the classical one) when the process mean is overestimated.

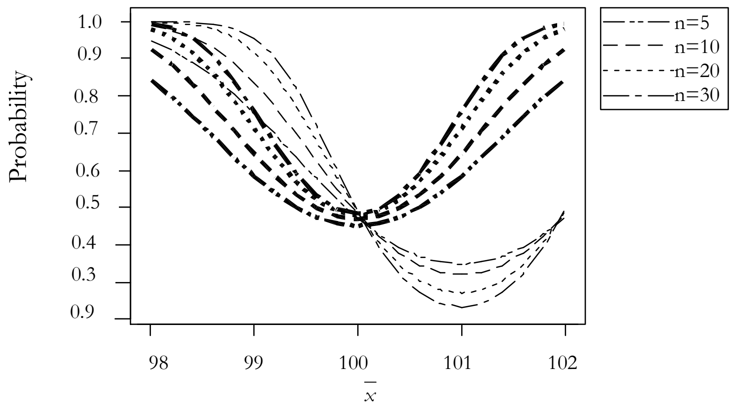

Figure 15. The *P*-value and α_0 under various sample means when $T = 101$, $\mu = 100$, and $\hat{\sigma}^2 = \sigma_0^2 = 5$.

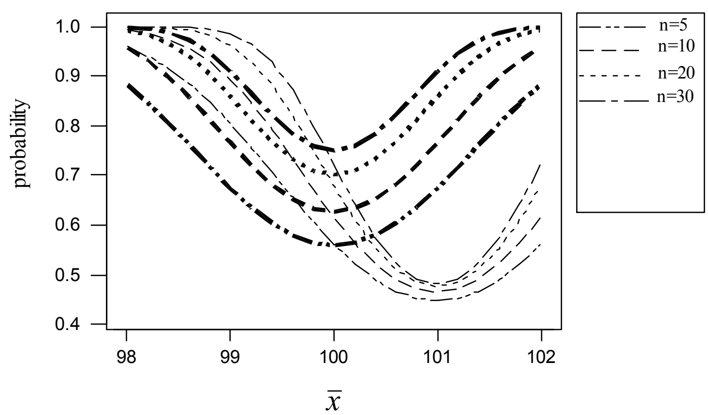

Figure 16. The *P*-value and α_0 under various sample means when $T = 99$, $\mu = 100$, and $\hat{\sigma}^2 = \sigma_0^2 = 5$.

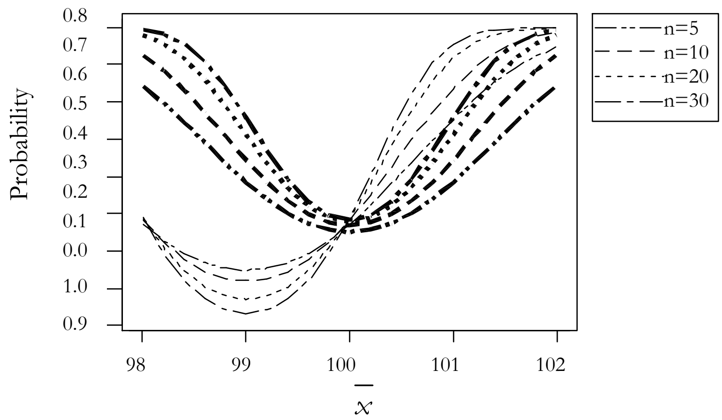

Figure 17. The *P*-value and α_0 under various sample means when $T = 101$, $\mu = 100$, $\sigma_0^2 = 5$, and $\hat{\sigma}^2 = 6$.

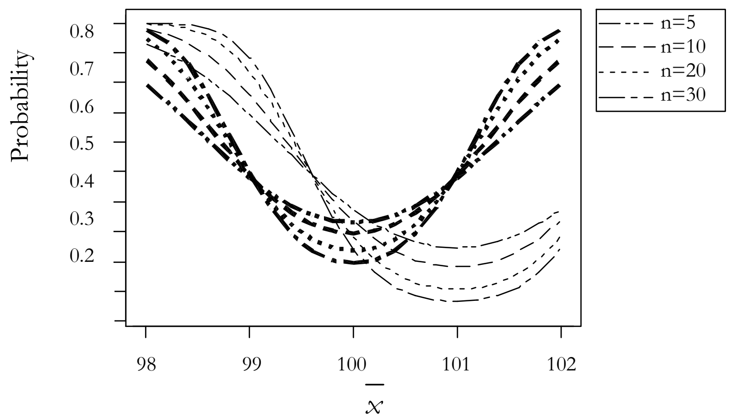

Figure 18. The *P*-value and α_0 under various sample means when $T = 101$, $\mu = 100$, $\sigma_0^2 = 5$, and $\hat{\sigma}^2 = 4$.

6. CONCLUSIONS AND FURTHER RESEARCH

Summary

Of late, process capability analysis has become one of the most rapidly growing segments of quality and productivity improvement and been coming into widespread use in practice. The process capability index Cpm was initially introduced by Chan et al. (1988), followed by Boyles (1991), which is one of the process capability measures that enable to evaluate the ability of a process to arrive at a pre-specified target value and to fall within the production specification simultaneously. In the first part of the paper, attention is restricted to the construction of credible intervals for the Taguchi capability index so that a noninformative prior belief depending on Fisher's information is assumed on the process variance to derive the posterior distribution $\pi(\sigma'|X)$, and subsequently the posterior probability of C_{pm} can conveniently be expressed as a gamma distribution. Based upon the notion of HPD regions in the Bayesian context, the Newton's method is utilized for univariate root-finding to anchor the HPD credible set (i.e., k_1 and k_2 in Figure 2), and via the variable transformation in (12), the HPD credible interval for C_{pm} is numerically obtained. The experimental study of the developed Bayesian HPD credible intervals for C_{pm} in comparison with classical confidence intervals demonstrates that the Bayes' interval estimator performs considerably better than the classical one pertaining to the sampling theory when the departures of the process mean from the target value are taking place. If the process center is located right on the target value, then the Bayesian and classical interval estimators are almost identical in all shapes and sizes (see Figure 3). The relevant computational results of these two interval estimators under a range of degrees of departure and numerous sample sizes are also reported in detail.

Furthermore, a Bayesian procedure established by the posterior distribution of C_{pm} for hypothesis testing of the Taguchi process capability is addressed as well. For comparison purposes, the significance probability α_0 provided by the Bayesian method is compared with the *P*-value generated by the classical sampling distribution approach while testing the process capability hypothesis (24). It has been proved that the *P*-value equals α_0 when the process mean is on the target value. To envision the competitive edges of these two testing procedures, a series of pictorial illustrations plotted under a wide variety of process parameter configurations are presented. The computational experience posed in Section 5 clearly advises us when and under what circumstances the Bayesian testing alternative should be adopted instead of the classical testing procedure. Another valuable facet of the proposed Bayes' solution (to interval estimate building and/or hypothesis testing) is due to its straightforward numerical computation, simply involving the gamma distribution and Newton's method. The well-known distributions and engineering techniques that the general engineers are more familiar with can readily be calculated and implemented in ordinary spreadsheet packages.

Directions for future research

Building upon this research, there are a number of interesting topics that deserve further research in this area. For instance, it would be challenging but very useful to investigate the Bayesian alternative means for constructing the interval estimate on the Taguchi process capability index when the normality assumption made on the process measurement data is seriously violated. Of practical relevance is the case of the process measurements being lognormal, which should belong to a separate study. The discussion in this paper is centered on the index C_{pm}. It is of interest to study the performance of the Bayesian-based approach on more advanced indices, such as C_{pmk} discussed in Pearn et al. (1992) and Jessenberger and Weihs (2000).

REFERENCES

1. Berger, J.O. (1988). *Statistical Decision Theory and Bayesian Analysis*, 2nd ed., Springer-Verlag, New York, NY.
2. Boyles, R.A. (1991a). The taguchi capability index. *Journal of Quality Technology*, 23(1): 17-26.
3. Boyles, R.A. (1991b). Corrigenda. *Journal of Quality Technology*, 23(4): 382.
4. Chan, K.L., Cheng, S.W., and Spiring, F.A. (1988). A new measure of process capability: C_{pm}. *Journal of Quality Technology*, 20(3): 162-175.
5. Cheng, S.W. and Spiring, F.A. (1989). Assessing process capability: a bayesian approach. *IIE Transactions*, 21(1): 97-98.
6. Chou, Y.M. and Owen, D.B. and Borrego, S.A. (1990). Lower confidence limits on process capability indices. *Journal of Quality Technology*, 22(3): 223-229.
7. Conte, S.D. and de Boor, C. (1980). *Elementary Numerical Analysis: An Algorithm Approach*, *3rd* ed., McGraw-Hill, New York, NY.
8. Deleryd, M. and Vannman, K. (1999). Process capability plots—a quality improvement tool. *Quality and Reliability Engineering International*, 15: 213-227.
9. Franklin, L.A. and Wasserman, G.S. (1992). Bootstrap lower confidence limits for capability indices. *Journal of Quality Technology*, 24(4): 196-210.
10. Jessenberger, J. and Weihs, C. (2000). A note on the behavior of C_{pmk} with asymmetric specification limits. *Journal of Quality Technology*, 32(4): 440-443.
11. Johnson, T. (1992). The relationship of C_{pm} to squared error loss. *Journal of Quality Technology*, 24(4): 211-215.
12. Juran, J.M., Gryna, F.M., and Bingham, R.S. (1979). *Quality Control Handbook*, McGraw-Hill, New York, NY.
13. Kane, V.E. (1986a). Process capability indices. *Journal of Quality Technology*, 18(1): 41-52.
14. Kane, V.E. (1986b). Corrigenda. *Journal of Quality Technology*, 18(4): 255.
15. Kotz, S. and Johnson, N.L. (1993). *Process Capability Indices*, Chapman and Hall, London.
16. Kotz, S. and Johnson, N.L. (2002). Process capability indices—A Review, 1992-2000 (with discussions). *Journal of Quality Technology*, 34(1): 2-53.
17. Kushler, R.H. and Hurley, P. (1992). Confidence bounds for capability indices. *Journal of Quality Technology*, 24(4): 188-195.
18. Lee, P.M. (1989). *Bayesian Statistics: an introduction, Oxford University Press*, New York, NY.
19. Montgomery, D.C. (2001). *Introduction to Statistical Quality Control*, *4th* ed., John Wiley *&* Sons, New York, NY.
20. Robert, C.P. (1994). *The Bayesian Choice: A Decision-Theoretic Motivation*, Springer-Verlag, New York, NY.
21. Shiau, J.H., Chiang, C.T., and Hung, H.N. (1999). A bayesian procedure for process capability assessment. *Quality and Reliability Engineering International*, 15: 369-378.
22. Spiring, F.A. (1991). Assessing process capability in the presence of systematic assignable cause. *Journal of Quality Technology*, 23(2): 125-134.
23. Spiring, F.A. (1997). A unifying approach to process capability indices. *Journal of Quality Technology*, 29(1): 49-58.
24. Sullivan, L.P. (1984). Reducing Variability—*A New Approach to Quality. Quality Progress*, 17(6): 15-21.
25. Sullivan, L.P. (1985). Letter. Quality Progress, 18(4): 7-8.
26. Taguchi, G. (1986). *Introduction to Quality Engineering*, Asian Productivity Organization, Tokyo, Japan.
27. Zimmer, L.S. and Hubele, N.F. (1997). Quantiles of the sampling distribution of C_{pm}. *Quality Engineering*, 10: 309-329.
28. Zimmer, L.S., Hubele, N.F. and Zimmer, W.J. (2001). Confidence intervals and sample size determination for C_{pm}. *Quality and Reliability Engineering International*, 17: 51-68.

APPENDIX A: JEFFREYS' NONINFORMATIVE PRIOR DISTRIBUTION $\pi(\sigma^2)$

For the unknown normal variance 2 with constant mean, the log-likelihood is

$$\log L\left(\sigma^2 \middle| x_i\right) = -\log\sigma - \frac{\left(x_i-\mu\right)^2}{2\sigma^2} + \text{constant}$$

so that

$$\frac{\partial^2 \log L\left(\sigma^2 \middle| x_i\right)}{\partial^2\sigma^2} = \frac{1}{2\sigma^4} - \frac{\left(x_i-\mu\right)^2}{2\sigma^6}$$

which does not depend on x_i. The *Fisher's Information* $I(\sigma^2)$ is

$$I\left(\sigma^2\right) = -E\left[\frac{\partial^2 \log f\left(x_i \middle| \sigma^2\right)}{\partial^2\sigma^2}\right] = -E\left[\frac{1}{2\sigma^4} - \frac{\left(x_i-\mu\right)^2}{\sigma^6}\right]$$
$$= -\frac{1}{2\sigma^4} + \frac{E\left(x_i-\mu\right)^2}{\sigma^6} = -\frac{1}{2\sigma^4} + \frac{\sigma^2}{\sigma^6} = \frac{1}{2\sigma^4}.$$

Hence, the Jeffreys' prior for σ^2 is

$$\pi\left(\sigma^2\right) \propto \sqrt{I\left(\sigma^2\right)} \propto \frac{1}{\sigma^2};\ 0 < \sigma^2 < \infty.$$

APPENDIX B: THE POSTERIOR DISTRIBUTION $\pi(\sigma^2 | X)$

From Bayes' Theorem, the posterior distribution of σ^2 is given as

$$\pi\left(\sigma^2 \middle| X\right) \propto \left(\sigma^2\right)^{-\frac{n}{2}} \exp\left[-\frac{\sum_{i=1}^{n}\left(x_i-\mu\right)^2}{2\sigma^2}\right]\left(\frac{1}{\sigma^2}\right)$$
$$\propto \left(\sigma^2\right)^{-\left(\frac{n}{2}+1\right)} \exp\left[-\frac{\sum_{i=1}^{n}\left(x_i-\mu\right)^2}{2\sigma^2}\right]$$
$$\propto \left(\sigma^2\right)^{-\left(\frac{n}{2}+1\right)} \exp\left[-\frac{\sum_{i=1}^{n}\left(x_i-\bar{x}\right)^2 + n\left(\bar{x}-\mu\right)^2}{2\sigma^2}\right]$$
$$\propto \left(\sigma^2\right)^{-\left(\frac{n}{2}+1\right)} \exp\left[-\frac{\left(n-1\right)\hat{\sigma}^2 + n\left(\bar{x}-\mu\right)^2}{2\sigma^2}\right],$$

where $\hat{\sigma}^2 = \sum_{i=1}^{n}\left(x_i-\bar{x}\right)^2 / (n-1)$.

In order to ensure that $\pi(\sigma^2 | X)$ is normalized to unit probability, it needs to compute the following integration by letting $t = \sigma^{-2}$

$$\int_0^\infty \left(\sigma^2\right)^{-\left(\frac{n}{2}+1\right)} \exp\left[-\frac{\left(n-1\right)\hat{\sigma}^2 + n\left(\bar{x}-\mu\right)^2}{2\sigma^2}\right] d\sigma^2$$
$$= \int_0^\infty t^{\frac{n}{2}-1} \exp\left[-\frac{\left(n-1\right)\hat{\sigma}^2 + n\left(\bar{x}-\mu\right)^2}{2} t\right] dt$$
$$= \Gamma\left(\frac{n}{2}\right)\left(\frac{2}{\left(n-1\right)\hat{\sigma}^2 + n\left(\bar{x}-\mu\right)^2}\right)^{\frac{n}{2}}.$$

Accordingly, the posterior distribution $\pi(\sigma^2 | X)$ in (9) follows from noting that

$$\pi(\sigma^2 | X) = \frac{\pi(\sigma^2) \times L(\sigma^2 | X)}{\int \pi(\sigma^2) \times L(\sigma^2 | X)\, d\sigma^2}.$$

APPENDIX C: THE DERIVATION OF α_1

$$\alpha_1 = \Pr[C_{pm} > c_0 | X] = \int_{c_0}^{\infty} \pi\left(C_{pm} \middle| X\right) dC_{pm}$$
$$= \int_0^A \pi\left(\sigma' \middle| X\right) d\sigma'$$

where

$$c_0 = \frac{\text{USL} - \text{LSL}}{6\sqrt{\sigma_0^2 + (\mu - T)^2}}, \quad \text{and} \quad A = \sqrt{\sigma_0^2 + (\mu - T)^2}.$$

Observing Equation (11) yields

$$\alpha_1 = \int_{c_0'}^{\infty} Gamma\left(y; \alpha = \frac{n}{2}, \beta = 1\right) dy,$$

where

$$c_0' = \frac{\left(n-1\right)\hat{\sigma}^2 + n\left(\bar{x}-\mu\right)^2}{2\left[\left(\sqrt{\sigma_0^2 + (\mu-T)^2}\right)^2 - \left(\mu - T\right)^2\right]}$$
$$= \frac{\left(n-1\right)\hat{\sigma}^2 + n\left(\bar{x}-\mu\right)^2}{2\sigma_0^2} = \frac{\chi^2_{n,\lambda'}}{2}\frac{\sum_{i=1}^{n}\left(x_i-\mu\right)^2}{\sum_{i=1}^{n}\left(x_i-T\right)^2},$$

where $\chi^2_{n,\lambda'} = [(n-1)\hat{\sigma}'^2]/\sigma_0^2$.

APPENDIX D

Corollary 1. When $\mu = T$, P-value in (29) is equal to α_0 in (33).

Proof. Rearranging terms in c_0' gives

$$c_0' = \frac{(n-1)\hat{\sigma}^2 + n(\bar{x}-\mu)^2}{2\sigma_0^2}$$

$$= \frac{\sum_{i=1}^{n}(x_i-\bar{x})^2 + n(\bar{x}-\mu)^2}{2\sigma_0^2} = \frac{\sum_{i=1}^{n}(x_i-\mu)^2}{2\sigma_0^2} .$$

By letting $t = 2y$, α_0 in (33) can be written as

$$\alpha_0 = \int_0^{c_0'} \frac{1}{\Gamma\left(\frac{n}{2}\right)} y^{\frac{n}{2}-1} e^{-y} dy = \int_0^{2c_0'} \frac{1}{2\Gamma\left(\frac{n}{2}\right)} \left(\frac{t}{2}\right)^{\frac{n}{2}-1} e^{-\frac{t}{2}} dt$$

$$= \int_0^{2c_0'} \frac{1}{\Gamma\left(\frac{n}{2}\right) 2^{\frac{n}{2}}} t^{\frac{n}{2}-1} e^{-\frac{t}{2}} dt = \int_0^{2c_0'} Gamma\left(t;\ \frac{n}{2},\ 2\right) dt$$

$$= \Pr\left[\chi_n^2 < 2c_0'\right]$$

$$= \Pr\left[\chi_n^2 < \frac{\sum_{i=1}^{n}(x_i-\mu)^2}{\sigma_0^2}\right],$$

which completes our proof.